

## ***SUB-MINIATURE ExB SECTOR FIELD MASS SPECTROMETER***

***Jorge A. Diaz<sup>†,‡</sup>, Clayton F. Giese<sup>‡</sup> and W. Ronald Gentry<sup>‡</sup>***

*<sup>†</sup>Universidad de Costa Rica, San Jose, COSTA RICA*

*<sup>‡</sup>University of Minnesota, Minneapolis, MN, USA*

### ***Abstract***

*A novel sub-miniature double-focusing sector field mass spectrometer has been fabricated at the University of Minnesota using a combination of conventional machining methods and thin film patterning techniques typically used in the sensor technology industry. Its design is based on the mass separation capabilities of a 90° cylindrical crossed electric and magnetic sector field analyzer with a 2cm radius, which under proper conditions is able to effectively cancel the angular and chromatic dispersion of the ion beam, thus improving the resolving power of the instrument. Ion simulations using finite element analysis and computer modeling were employed to verify and optimize the performance of the proposed instrument before and during its fabrication. The prototype was able to attain a resolving power of 106 (FWHM), a detection limit close to 10 parts per million, a dynamic range of 5 orders of magnitude and a mass range up to 103 atomic mass units. Its overall size, including the magnet assembly, is 3.5cm wide, 6 cm long and 7.5 cm tall, it weighs 0.8 kg, and its power consumption was measured to be 2.5 W. Its performance was found to be comparable to commercial residual gas analyzers at a fraction of the cost. All these characteristics make this miniature mass spectrometer suitable for portable and low cost analytical instrumentation.*

### **I. Introduction**

Among all the possible analytical instruments, few are more powerful and have a wider range of applications than mass spectrometers (MS). Despite all their capabilities, traditional mass spectrometers do have several limitations. The major disadvantage of mass spectroscopy as an analytical technique is the complexity of the instrumentation required and its associated cost. Although some special-purpose MS are available with prices in the \$10,000 range, as in the case of Residual Gas Analyzers (RGA), the typical cost of a general-purpose analytical MS is \$100,000 up to \$1,000,000 in the case of very high resolution instruments. The components, such as sample inlet, ion source, mass analyzer, detector housing and vacuum envelope are typically manufactured by conventional machining techniques, assembled and aligned manually, and finally each one is individually tuned and calibrated to meet the manufacturer's product specification. Due to the number of independent pieces and the elaborate geometry of typical MS, the manufacturing process is not compatible with mass production techniques. Also, commercially available instruments require high vacuum systems to operate, and usually possess high voltage and high power operating requirements. Furthermore, the operation and maintenance of such an instrument typically requires the full-time effort of a highly trained scientist or technician.

All of these requirements hinder the use of this powerful technique in applications that require a reliable, low-cost, small and portable analytical sensor. Likewise, due to these constraints, in the case of applications such as environmental sampling, traditional mass spectrometers are not suitable for "in situ" measurements.



**Figure 1. Compact Double Focusing Mass Spectrometer (CDFMS) Core**

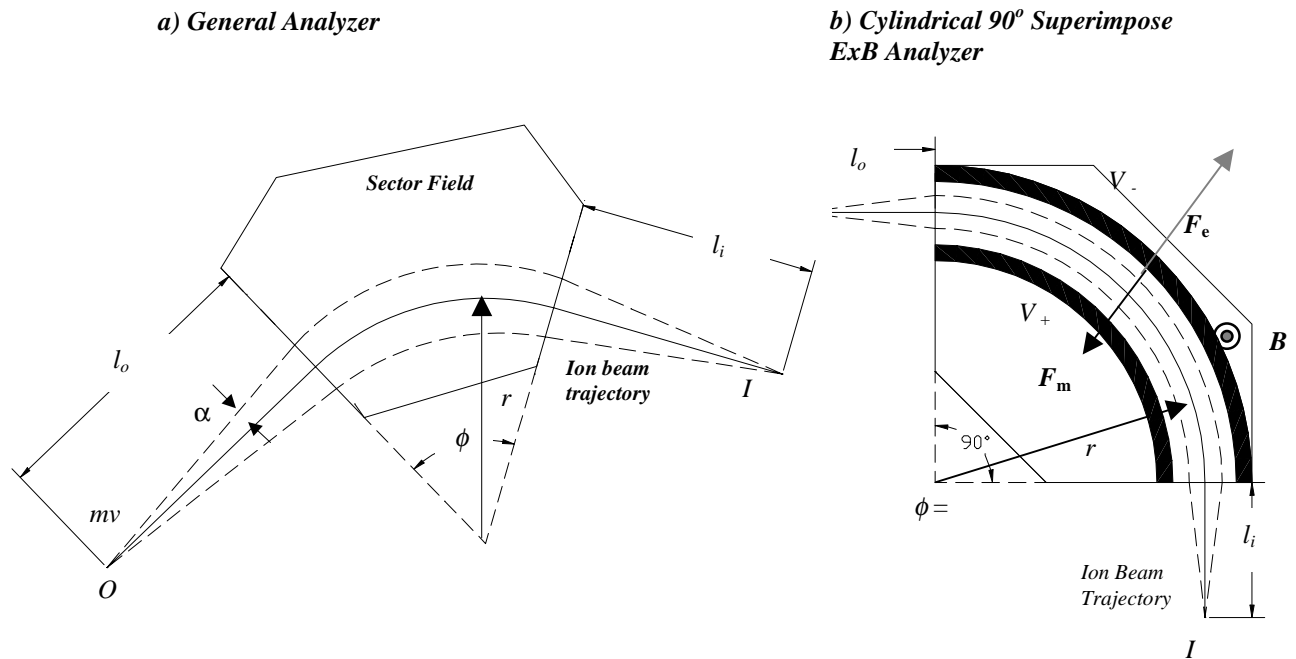


**Figure 2. Sector Field Ion Focusing**

We began this research project with the belief that the complexity and hence the cost of analytical mass spectroscopy can be drastically reduced, to permit this powerful technique to be used in applications where it has previously not been practical or cost-effective. By the appropriate choice of design, together with the use of finite element analysis ion optics simulations, we thought that the weight and size might be reduced from one to several orders of magnitude in comparison with existing mass spectrometers. This, in conjunction with the use of new materials and modern mass production manufacturing techniques, could lead to a new generation of simpler, smaller, more reliable and much less costly mass spectrometers for general analytical applications. Following this course of action we have developed a novel miniature mass spectrometer (Figure 1) that we call the *Compact Double-Focusing Mass Spectrometer (CDFMS)*. The resulting design is small, lightweight, and has low power consumption. It can also be made compatible with mass production manufacturing techniques, making this new instrument suitable for a wide variety of applications where continuous and real time on-site monitoring of mass spectral data is required.

## II. Instrument Design

The design of the CDFMS is based on the mass separation and focusing capabilities of sector field analyzers—more specifically a  $90^\circ$  double-focusing mass analyzer using cylindrical crossed electric and magnetic fields<sup>(1)</sup>.

### A. Background

In mass spectrometry, *double focusing* is achieved when ions emerging from an ion source with spreads in both *energy* and *direction* are efficiently focused to points in space which depend only on the ion mass in first order. Under this condition, the resolving power of the mass spectrometer can be much greater than in single-focusing instruments that provide direction-focusing only.

For sector field instruments, *direction focusing* can be achieved using magnetic fields alone<sup>(2)</sup>. Magnetic field mass analyzers are capable of separating the ions by their  $m/z$  ratio and bringing them to focus at the detector slit. On the other hand, *energy focusing* in a sector analyzer requires the use of electric fields<sup>(3)</sup>. Traditionally, electric and magnetic sectors are placed in tandem to create a double-focusing mass spectrometer.<sup>(4,5,6)</sup>

Another way to obtain double focusing of the ion beam is by superimposing electric and magnetic fields with vector directions perpendicular to each other. This kind of geometrical arrangement is called

*Crossed Electric and Magnetic Field or ExB Superimposed Field* and has been used in the design and construction of Wien filters, cycloidal mass spectrometers<sup>(7)</sup> and ion cyclotron resonance mass spectrometers<sup>(8)</sup>. These three types of crossed field analyzers have been employed in various small mass spectrometers, for example: a 2 cm 180° magnetic analyzer with Wien filter<sup>(9)</sup>, a miniature (2.7 cm from slit to detector) cycloidal focusing mass spectrometer<sup>(10)</sup>, a compact (1 cm radius) helium detector<sup>(11)</sup>, and a back-pack portable ion cyclotron resonance MS<sup>(12)</sup>

Very few mass spectrometers have been designed with cylindrical *ExB* superimposed fields having double focusing capabilities. In this design, the radial electric field of cylindrical symmetry is superimposed at right angles to the homogeneous magnetic field, and double focusing is achieved only with a special ratio of  $E/B$ . Bartky and Dempster<sup>(13)</sup> were the first to propose such an arrangement for the specific case of an homogeneous magnetic field placed perpendicular to a cylindrical condenser, with ions

travelling through the crossed fields and focusing at a deflection angle of  $\frac{\pi}{\sqrt{2}}$  rad (127.3°). Based on this

design, Bondy and Popper<sup>(14)</sup> built a 127.3° superimposed *ExB* mass spectrometer having the detector and the ion source located at the field boundaries. They were able to achieve a resolving power ( $RP$ ) of 380 at mass 23 amu ( $\text{Na}^+$ ). They later used the apparatus to measure the relative isotopic abundances of potassium ( $^{39}\text{K}$ ,  $^{41}\text{K}$ ) and rubidium ( $^{85}\text{Rb}$ ,  $^{87}\text{Rb}$ )<sup>(15)</sup>. The analyzer was relatively small ( $r = 4\text{cm}$ ), but the instrument operated at a constant accelerating voltage (100V) with sweeping of the magnetic field and thus requiring a very large electromagnet.

The general properties of crossed electric and magnetic fields having cylindrical symmetry, for both homogeneous and inhomogeneous magnetic field cases, were first summarized by Fisher<sup>(16)</sup>. He established the universal formulas for dispersion, resolution, resolving power and beam spread for such analyzers and provided mathematical descriptions of some basic experimental configurations. Parallel to his mathematical treatment, Fisher built another 127.3° cylindrical *ExB* analyzer<sup>(17)</sup> similar to Bondy and Popper's spectrometer but with a radius of 14 cm and higher accelerating voltage ( $V = 1000\text{V}$ ). He used the apparatus to study the focal properties of this kind of analyzer under different field conditions and was able to measure the neon isotopes ( $^{20}\text{Ne}$ ,  $^{22}\text{Ne}$ ) with a resolving power close to 240.

Matsuda<sup>(18)</sup> further developed the mathematical treatment of the crossed electric and magnetic field analyzer, including special electric field shapes to achieve directional focusing in both the plane of deflection and perpendicular to this plane. He also introduced the 90° cylindrical *ExB* analyzer with image and object focal points outside of the sector field boundaries. He fabricated a large mass spectrometer using this geometry<sup>(19)</sup>. He and his collaborators used the crossed analyzer in tandem with a cylindrical energy analyzer<sup>(20)</sup>, running the ion beam at a constant accelerating voltage and compensating for the

change of the focal point by modifying the electric field shape with a pair of plates (Matsuda plates) placed above and below the cylindrical electrodes<sup>(21,22)</sup>. Double focusing was not obtained by the crossed-field mass analyzer itself, but with the second energy analyzer. With this configuration, they were able to achieve mass spectra with high resolution ( $RP \approx 1000$ ). Although Matsuda suggested the use of the  $90^\circ$  crossed sector field to realize a double focusing mass spectrometer, the device was mainly employed for MS/MS applications<sup>(23)</sup> in which the accelerating voltage was kept constant and chromatic focusing was obtained by separate cylindrical energy analyzers. Naito<sup>(24)</sup> also proposed an  $ExB$  analyzer running at constant voltage  $V$ , but with either a quadrupole lens or another  $ExB$  field arranged in tandem with the first superimposed sector to compensate for the change of in focal length.

Because of the compact geometry and the double focusing capabilities that the  $90^\circ$  cylindrical  $ExB$  sector field analyzer offers, we used this principle in developing a miniature mass spectrometer targeted for gas monitoring applications. To our knowledge, this is the first time this particular configuration has been used on a miniature mass spectrometer<sup>25</sup>

### ***B. Ion Focusing Principles***

In a typical mass spectrometer, the ion source focuses the beam into the entrance slit, and the resulting ion beam enters the analyzer region with both direction and energy spreads. The mathematical treatment of the ion trajectories associated with sector fields was summarized by Mattauch and Herzog<sup>(26), (27)</sup>. The sector could be a radial electric field, a homogeneous magnetic field or a combination of both in the same space. Figure 2 defines the parameters for ions travelling through such a sector field analyzer. For a general sector field (Figure 2a), the ions of mass  $m$ , exit the object point "O" with velocity  $v$  and half angular spread  $\alpha$ , at a distance  $l_o$  from the field boundary. The ions enter normal to the field boundary and are deflected through an angle  $\phi$ , in a circular path of radius  $r_o$ . The ions exit the field normal to the boundary and are focused at position "I" after travelling a distance  $l_i$ . The system satisfies the following ion optics equations:

$$(l_o - g)(l_i - g) = f^2 \quad (1)$$

$$f = r_o / [k_r \sin(k_r \phi)] \quad (2)$$

$$g = f \cos(k_r \phi) = r_o / [k_r \tan(k_r \phi)] \quad (3)$$

where

- $l_o$  : object distance (source slit to field boundary);
- $l_i$  : image distance (detector slit to field boundary);
- $f$  : system's focal length (characteristic of the specific sector field);
- $g$  : distance between field boundary and principal focus;
- $k_r$  : constant (depends on the particular field being used).

If the source and the detector are placed symmetrically with respect to the field boundaries ( $l_o = l_i$ ), from equations (1), (2) and (3), directional focusing of the ion beam will occur at:

$$l_{o,i} = f + g = \left( \frac{r_o}{k_r} \right) [ \csc(k_r \phi) + \cot(k_r \phi) ] \quad (4)$$

For the superimposed  $E \times B$  analyzer, the electric field  $E$  is oriented parallel to the radial vector  $\hat{r}$  and the magnetic field  $B$  is placed perpendicular to the electric field (Figure 2b). The signs of the electric and magnetic fields are chosen such that the forces from them are anti-parallel. From Matsuda<sup>(18)</sup>, if the electric and magnetic fields can be written in the form:

$$E_r = U_0 r^l \text{ and } B_z = B_0 \left( \frac{r_o}{r} \right)^n \quad (5)$$

Then,  $k_r$  can be expressed as:

$$k_r^2 = \frac{r^2}{r_m^2} + \left[ \left( 1 - \frac{r}{r_m} \right) \cdot (l + 3) + n \cdot \left( \frac{r}{r_m} \right) \right] \quad (6)$$

where  $r$  is the radius of the trajectory followed by an ion traversing the superimposed sector fields, and  $r_m$  is the radius of the same ion travelling through the same magnetic field but without the electric field. In our case  $r/r_m = 2$ . For a homogeneous magnetic field  $n = 0$ , and if the electric field is cylindrical,  $l = -1$ , and thus  $k_r^2 = 2$ . Substituting these values into equation (4) with  $\phi = 90^\circ$ , *directional focusing* occurs at:

$$l_o = l_i \approx 0.35 r \quad (7)$$

If a radial positive force is defined as inward and a negative force is outward along the radius of curvature, then the equation of motion of an ion of mass  $m$  is given by:

$$F = qBv - qE = \frac{mv^2}{r} \quad (8)$$

Solving for  $r$  we have:

$$r = \frac{mv^2}{qBv - qE} \quad (9)$$

In order to achieve energy focusing, the dispersion of  $r$  with respect to  $v$  inside the analyzer must be zero<sup>(28)</sup>. If  $E$  and  $B$  are kept constant for a particular mass, differentiating equation (9) with respect to  $v$ ,

will give:

$$\frac{dr}{dv} = \left( \frac{Bv - 2E}{Bv - E} \right) \frac{r}{v} \quad (10)$$

For *energy focusing*, we have the condition  $\frac{dr}{dv} = 0$  and thus  $Bv = 2E$ . Thus the magnetic force is twice the electric force or:

$$\left(\frac{F_m}{F_e}\right) = -2 \quad (11)$$

In summary, double-focusing of the ion beam with the crossed field analyzer will occur when the magnetic force is twice the electric force, and the focal points of the ion source and the detector slits are placed symmetrically a distance of 0.35 times the design radius from the sector field boundaries.

From Fischer<sup>(16)</sup>, the theoretical resolving power ( $RP_{Theory}$ ) for full-width at half-maximum (FWHM) for a superimposed  $ExB$  cylindrical analyzer with homogeneous magnetic field ( $n = 0$ ) is given by:

$$RP_{Theory} = \frac{m}{\Delta m} = \frac{2 \cdot r_o(1-l)}{\left((S_o + S_i) \cdot (1+l^2) + r_o(1+l) \frac{dV}{V}\right)} \quad (12)$$

In our case we have  $l = -1$ , then:

$$RP_{Theory} = \frac{m}{\Delta m} = \frac{2 \cdot r_o}{(S_o + S_i)} \quad (13)$$

where  $S_o$  and  $S_i$  are the widths of the entrance (object) and exit (image) slits of the analyzer.

### C. Geometry and Parameter Calculation

To meet our small size and portability goals, a radius ( $r_o$ ) of 2 cm was chosen for the first CDFMS analyzer. From equation (7), the positions of the object and image focal points are both 7 mm from the field entrance and exit boundaries.

If  $r_o$  is the fixed radius at the center of the cylindrical  $ExB$  analyzer and  $B$  is kept constant, the selected

mass is given by:

$$m = \frac{c_o}{V} \quad \text{with} \quad c_o = \frac{q B^2 r_o^2}{8} : \text{constant} \quad (14)$$

The mass spectrum is produced by sweeping the voltage over the range of the selected masses. To avoid the cumbersome use of electromagnets as in the case of previous cylindrical crossed field spectrometers, the magnetic field in our instrument is provided by permanent magnets. We designed the gap to be just 4mm tall.

If  $B = 1 \text{ Tesla}$  and  $r_o = 2 \text{ cm}$ , then the selected mass of singly charged ions for the CDFMS will be:

$$m (\text{amu}) = \frac{4824}{V} \quad (\text{Crossed DF Theory}) \quad (15)$$

The superimposed electric field sector is generated by two cylindrical plates 2.5 mm high, with radii  $r_+ = 0.95r_o = 19$  mm and  $r_- = 1.05r_o = 21$  mm . This creates a 2 mm cylindrical corridor where the mass separation takes place. As explained in the last section, to achieve double focusing, the direction of the electric field vector needs to be parallel to  $\hat{r}$  . Thus, the inner electrode is set to a voltage  $V_+$  higher than the outer electrode voltage  $V_-$  . The cylindrical electric field across the analyzer gap, assuming no fringing field effects, is given by:

$$E = \frac{k_o}{r}; \quad k_o = \text{constant} \quad (16)$$

Under double focusing conditions, from equation (9),  $r = \frac{2V}{E}$  . Therefore  $k_o = 2V$  . If the analyzer voltages are set such that the value of the equipotential at  $r_o$  is zero, then the voltage  $V_a$  inside the analyzer gap is:

$$V_a(r) = 2V \ln\left(\frac{r_o}{r}\right) \quad (17)$$

and the voltages at the cylindrical electrodes are both functions of the acceleration voltage  $V$ :

$$: \quad V_+ = V_a(r_+) = 0.1026 V \quad (18)$$

$$V_- = V_a(r_-) = -0.0976 V \quad (19)$$

#### ***D. Ion Simulations***

Using the expressions above and the proposed analyzer geometry, a computer model was created to simulate the trajectories of ions travelling through the  $90^\circ$  cylindrical  $ExB$  sector and to verify and optimize the mass separating capabilities of the small analyzer. The finite element modeling and analysis was done using SIMION 6.0<sup>(29)</sup>.

A two-dimensional (2D) model of the proposed analyzer was first created and the trajectory of  $m/z$  28 ions ( $N_2^+$  parent peak) through the analyzer were simulated. (Figure 3). From equations (15 ), (18) and (19), the required kinetic energy to select these ions is 172.3 eV ,with the cylindrical condenser plate voltages set to  $V_- = -16.82$  volts and  $V_+ = 17.68$  volts. We assumed a typical angular spread of  $6^\circ$  and at first no energy spread for the ions entering the analyzer

As depicted in Figure 3a, the analyzer was not able to bring the ion beam to a stigmatic focus. This is due to the fringing field effects, which are very critical for the dimensional scales involved in small mass spectrometers, and may ultimately define the performance of the instrument. The failure to address and to correct for such effects has been a very important limiting factor for most of the miniature mass

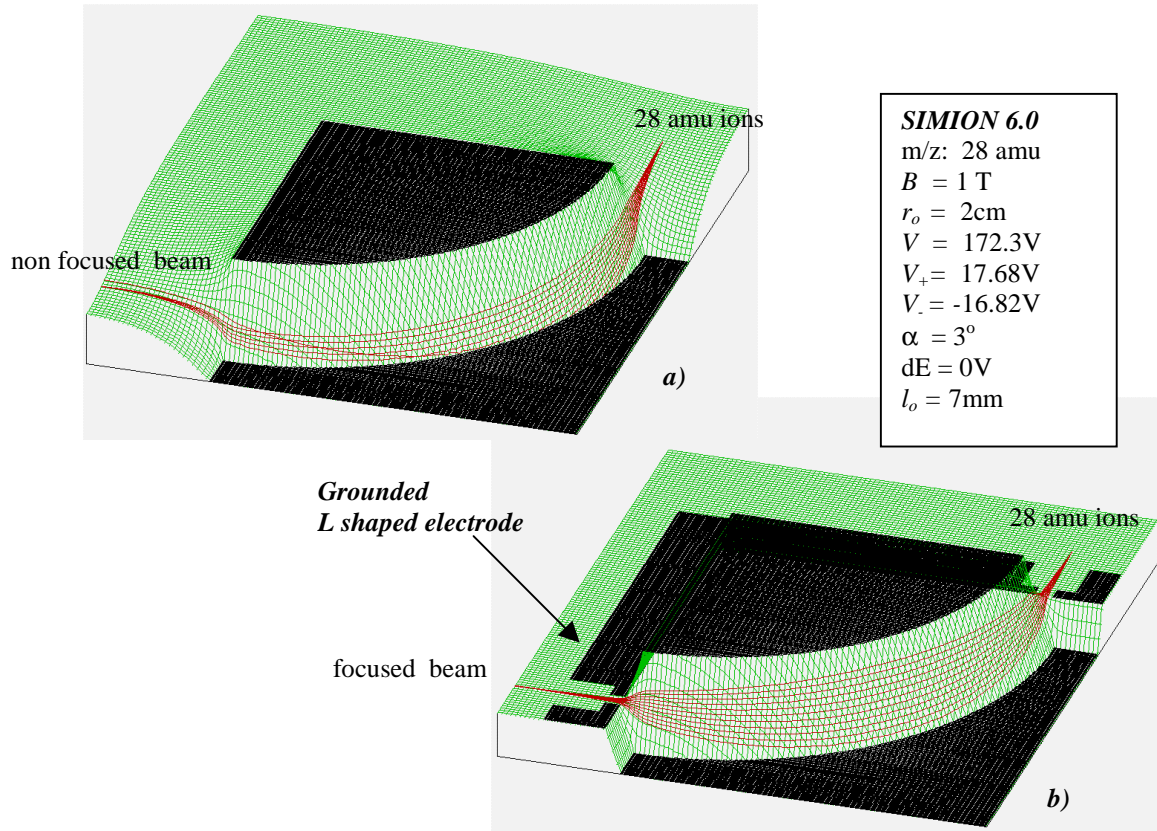


Figure 3: Entrance and Exit Electric Fringing Field Effects and Correction

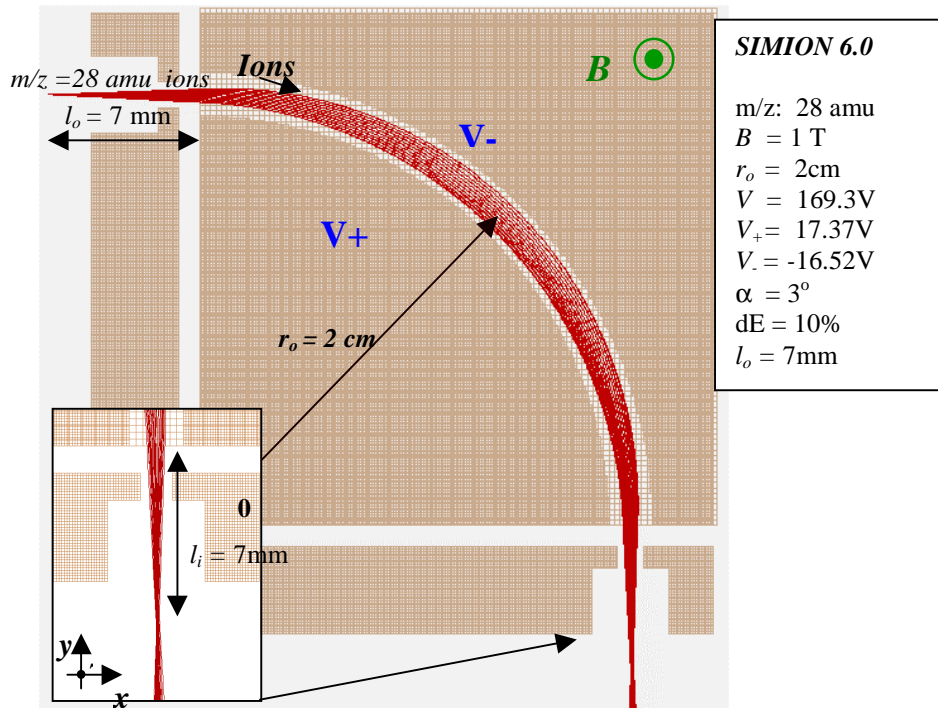


Figure 4: Mass 28 Double Focusing Verification

spectrometers built in the past. For large mass spectrometers, the corrections for fringing field effects have been commonly done in two ways. The first is to use a set of higher order focusing equations and to characterize the properties of the double focusing analyzers for different field conditions, shaping the trajectory of the ion beam and the fields to achieve very high resolution spectra<sup>(30)</sup>. The shortcoming of this method is the complexity involved in the numerical calculations and their experimental verification. The second way to correct the fringing field effects, and the one more traditionally used in the design and construction of mass spectrometers, is to add compensation lenses which are adjusted empirically to achieve the best resolution. This method is generally satisfactory for large mass spectrometers in which there is ample room along the ion path to install the correction lenses.

With the introduction of computer ion trajectory simulation packages, where the electric and magnetic field geometries can be designed and tested by FEA modeling before construction, the identification and correction of fringing field effects can be easily done without the necessity of finding analytical solutions to a large set of ion beam optical equations. Final empirical adjustment of the beam and fields may still be needed, but the iteration time is small.

To limit the electric field distortion in the xy plane at the entrance and exit of the analyzer, a grounded “L” shaped electrode is placed surrounding the analyzer at 1mm distance from the boundaries of the electric and magnetic sectors. (Figure 3b)

The change in the field boundary conditions makes the relationship between the accelerating voltage and selected mass (15) slightly different from that of the ideal field geometry. The updated ion trajectory model was used to determine the optimum kinetic energy to select  $m/z = 28$  amu ions and to detect them at the image position. The corrected set of voltages for  $m/z = 28$  amu were:  $V = 169.3$  volts,  $V^- = -16.52$  volts  $V^+ = 17.37$  volts, therefore:

$$m \text{ (amu)} = \frac{4740}{V}; \quad \text{(FE Ion Simulation)} \quad (20)$$

The next step was to confirm the double focusing capabilities of the 2cm 90° cylindrical *ExB* analyzer. The same ions and voltage settings as in Figure 3 were used, but instead of a monoenergetic beam of ions, an angular spread of 6° ( $\alpha = 3^\circ$ ) and kinetic energy spread ( $dE$ ) of 10% were assumed (Figure 4). The ions were focused in both direction and energy as predicted. In addition, the image focal point was verified to be 7mm away from the sector field boundary.

Once the performance of the scaled analyzer was characterized and the first set of operating parameters established, a complete 3D finite element model including the filament, ion source and detector slits was designed for the miniature mass spectrometer. The geometry for the CDFMS computer model is depicted in Figure 5.

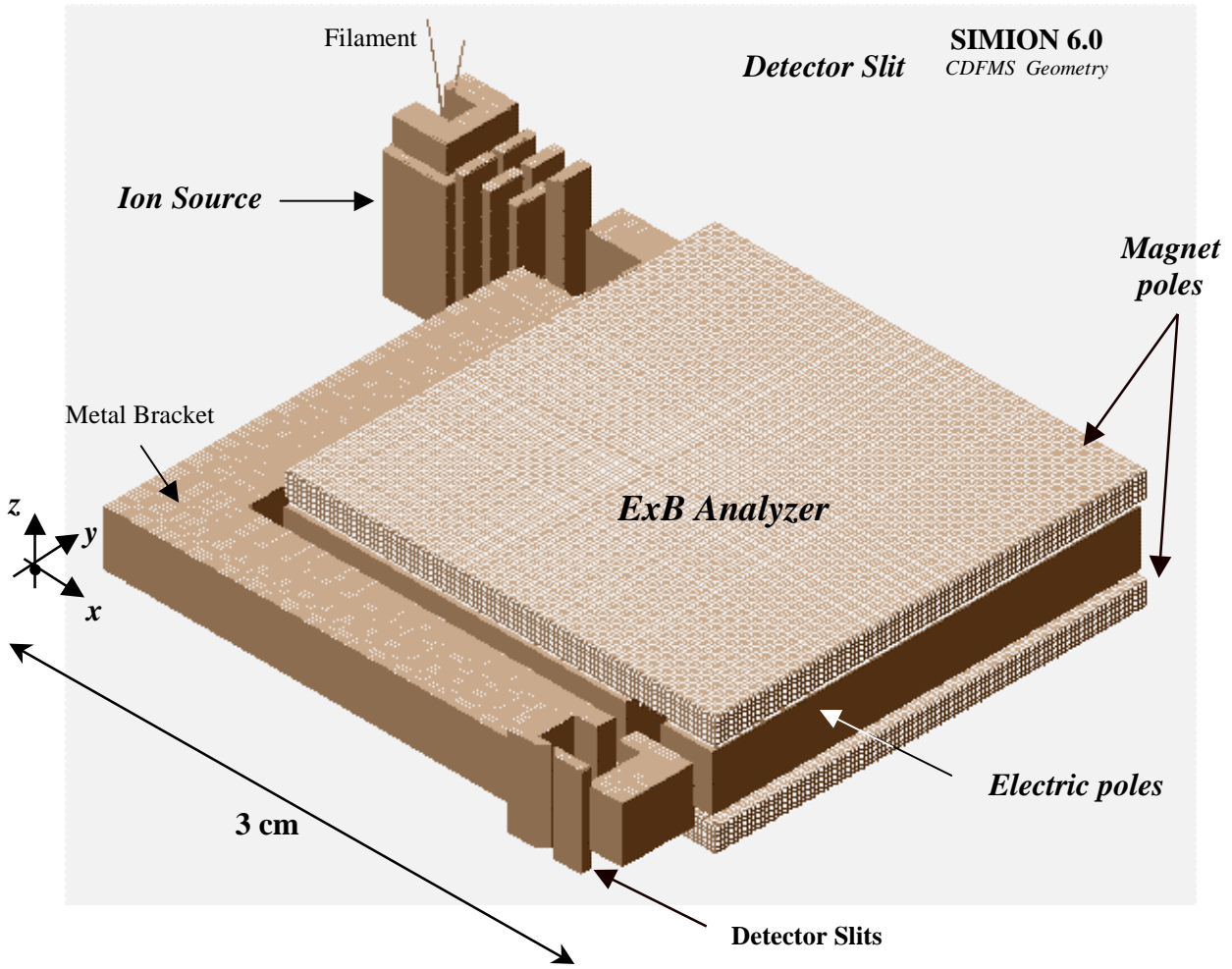


Figure 5: CDFMS Ion Simulation Model

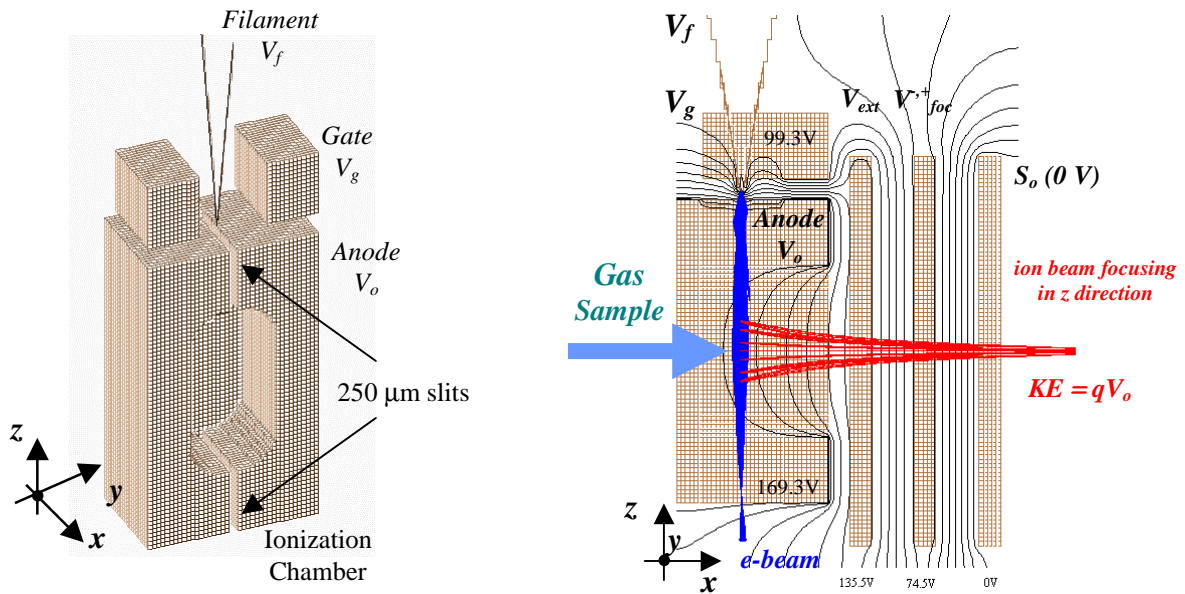


Figure 6: Ion Source Simulation

The ion source and the detector are placed at the designed separation distances from the sector field boundaries. The ion source consists of filament ( $V_f$ ), filament gate ( $V_g$ ), anode electrode ( $V_o$ ), ion extractor electrodes ( $V_{ext}$ ), focusing electrodes ( $V_{foc}^{+,-}$ ) and entrance electrodes (grounded). The anode electrode contains the ionization chamber and has slit apertures 250 $\mu$ m wide at its top and bottom to define the electrons beam. This e-beam is provided by a small hair-pin filament placed directly above the anode electrode and aligned parallel to the slit.. The filament electrode is mounted so as to make small changes in position possible. (Figure 6)

The CDFMS FE model simulates the electron beam produced by thermionic emission from a heated tungsten wire. The thermally emitted electrons are accelerated by the 70 volts potential difference between the filament  $V_f$  and the anode  $V_o$ . To avoid too much spread of the e-beam and to shield the influence of other electrodes on the filament, the gate electrode is designed to surround the filament with its voltage  $V_g$  set equal to  $V_f$ . Serendipitously, the fringing field produced by the permanent magnet provides effective collimation of the electron beam. The extractor, focusing and exit electrodes are 0.5mm thick, with a spacing of 1mm. The extractor plates are positioned 0.5 mm away from the ionization chamber and the entrance slit is placed flat against the grounded bracket. The width of the extractor and focusing slits is 0.7mm and that of the entrance slit is 0.2mm. The 9 mm height of the ion source electrodes is enough to approximate a parallel slit geometry, minimizing the electric fringing field effects at the top and bottom of the electrodes. In addition, the shape of the ionization chamber contributes to focusing of the beam in the z direction as seen in Figure 6.

With the ionization chamber set to  $V_o$  and the exit slit grounded, singly-charged ions are accelerated by the ion source electrodes to be injected into the analyzer with a kinetic energy close to  $eV_o$ , which makes:

$$V = V_o \text{ (FEA simulation)} \quad (21)$$

The computer model was used to find the proper set of extractor and focusing electrode voltages to achieve focusing of the ion beam with small angular dispersion in the xy plane and an acceptably low energy spread. The tuning of the simulated ion beam generated the following settings for the ion source:

$$V_f = V_g = V_o - 70 \text{ volts} \quad (22)$$

$$V_{ext} = 0.8 V_o \quad (23)$$

$$V_{foc}^+ = 0.44 V_o; V_{foc}^- = 0.40 V_o \quad (24)$$

The offset between the focusing electrodes ( $V_{foc}^+, V_{foc}^-$ ) was used to compensate for the effect on the ion trajectories from the magnetic fringing field present in the ion source.

From equations (20) and (21), the mass-to-charge ratio is selected by setting the anode voltage  $V_o$  to ( $m/4740$ ) volts. All the other electrode voltages, both at the ion source and analyzer, are directly

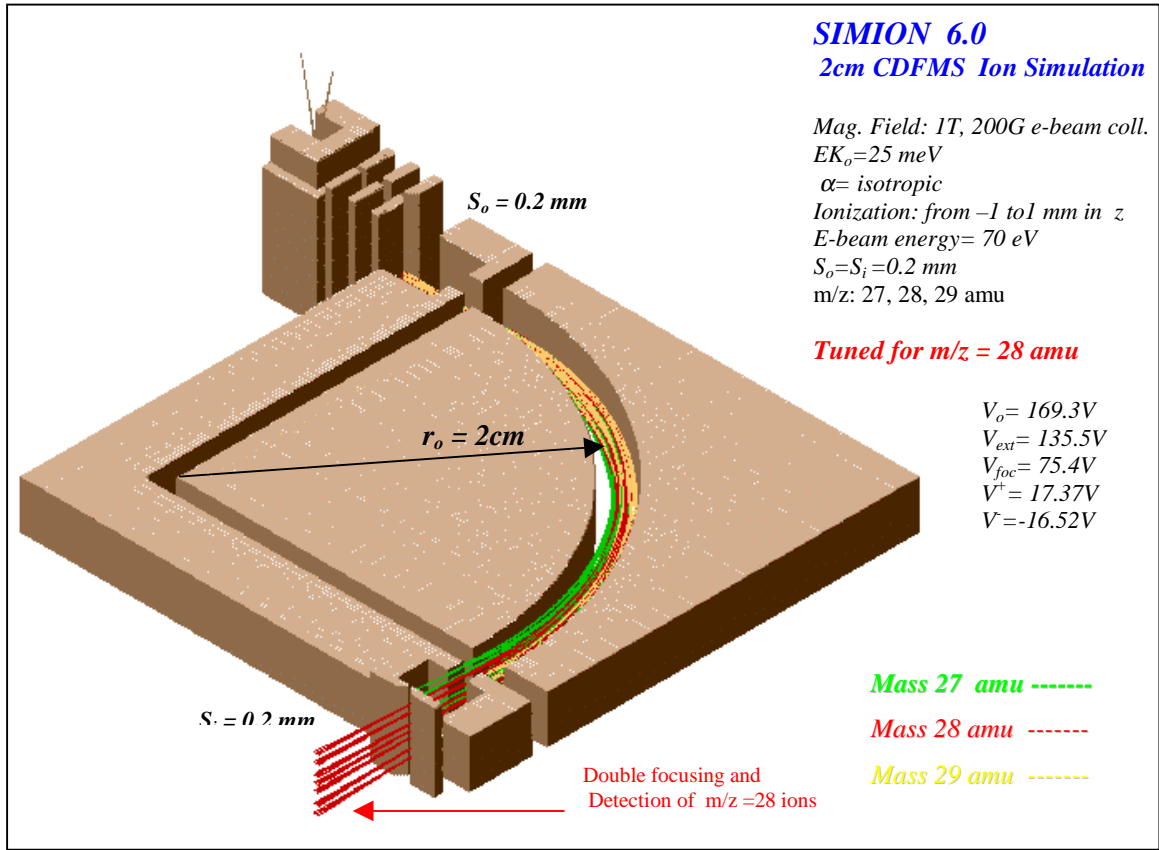


Figure 7: Miniature Mass Spectrometer 3D Ion Simulation for  $m/z = 27, 28$  and  $29 \text{ amu}$

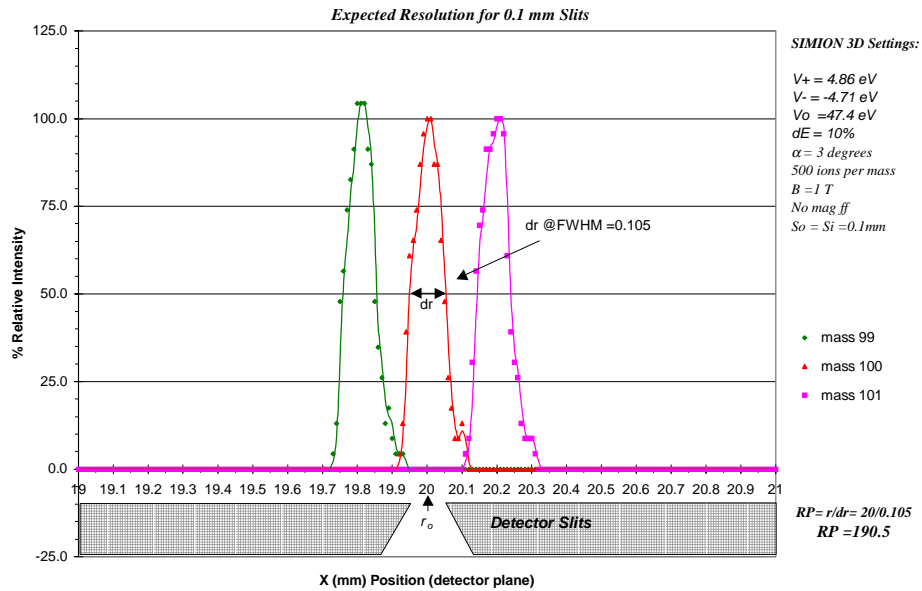


Figure 8: Mass Spectrum obtained using the CDFMS 3D Ion Simulation. ( $m/z = 27, 28$  and  $29 \text{ amu}$ )

proportional to this anode voltage. In this way, it is possible to acquire a mass spectrum by sweeping just one power supply voltage.

With the use of equations (18) through (24), the operating parameters to detect any mass-to-charge ratio can be calculated. For example, to measure  $m/z = 28$  amu with the simulated CDFMS design ( $r_o = 2\text{cm}$ ,  $B = 1.0\text{T}$ ), the operating voltages would be:

$$\text{Ion Source: } V_o=169.3\text{V}, V_f=V_g=99.3\text{V}, V_{ext}=135.5\text{V}, V_{foc}^+ = 74.5\text{V}; V_{foc}^- = 71.4\text{V}, \text{Slit} = 0\text{V}$$

$$\text{Analyzer: } V_+ = 17.37\text{V}, V_- = 16.52, \text{Bracket} = \text{Detector Slit} = 0\text{V}.$$

Using these settings, we simulated the trajectory of three different ions ( $m/z = 27, 28$  and  $29$  amu.) to evaluate the CDFMS performance (Figure 7). The simulation showed good focusing and mass separation.

A more complete study of the CDFMS resolving power was done using the finite element model, with  $m/z = 99, 100$  and  $101$  amu ions,  $0.1\text{mm}$  slits and the software features of SIMION 6.0. The settings were now changed to detect mass  $100$  while rejecting masses  $99$  and  $101$ . Five hundred ion trajectories per mass were simulated. The ion beam illuminated the  $0.1\text{mm}$  object slit ( $S_o$ ), entering the analyzer with about  $10\%$  spread in energy and  $6^\circ$  spread in angle. The  $90^\circ$  cylindrical  $ExB$  analyzer separated the incoming beam into the three different  $m/z$  ratios, achieving double focusing for each ion beam. The trajectory of each single ion was recorded and saved into a file, then the position of each ion when it reached the detector slit plane was extracted from the data. The  $2\text{mm}$  radial gap between the cylindrical electrodes at the detector was divided into  $100$  different bins each  $0.02$  mm wide. For each mass, the number of ions hitting that particular bin position was counted. By plotting ion counts versus bin position, we thus obtained a simulated mass spectrum resolved in space (Figure 8)

The simulated miniature mass spectrometer was able to resolve the three different ions satisfactorily. For mass  $100$ , the peak position was located at  $r = 20.005\text{mm}$  which was in close agreement with the design radius ( $20.000\text{mm}$ ). The radial dispersion  $dr = 0.105\text{mm}$  was measured for the same peak at full width of half maximum. The corresponding resolving power calculated from figure 10 is:

$$RP_{Simulation} = \frac{m}{dm} = \frac{r}{dr} = \frac{20.005}{0.105} = 190.5 \quad (25)$$

which is very similar to the simple theoretical value (see equation 13):

$$RP_{Theory} = \frac{2 \cdot r_o}{S_i + S_o} = \frac{2 \cdot 20.00}{0.20} = 200 \quad (26)$$

On the basis of these simulations, it appears that a CDFMS with  $2$  cm radius and  $0.1$  mm slits would be capable of a mass range and resolving power suitable for detection of most of the gas species commonly present in environmental gas samples.

### III Device Fabrication and Testing

Once the design of the CDFMS was established, the first prototype was fabricated with the help of numerically controlled machining (NCM) and thin film techniques. Figure 9 describes the different components of the CDFMS prototype. Copper (Cu) and stainless steel (SS) were used as conductive material for the electrodes, while Vespel<sup>®</sup> and Teflon<sup>®</sup> were used for the insulators. The ion beam electrodes and their respective insulators were designed to self-align when mounted to the bracket. Commercially available<sup>(31)</sup> slits were used. Connections to the plates were provided by directly soldering 20-gauge wires to them, or by brass connectors placed on the mounting screws. The SS anode contained an ionization chamber 4mm long, 2mm wide and 3 mm deep, and the electron beam was injected through a 250  $\mu\text{m}$  slit. The gas sample was introduced to the ionization chamber through a 250  $\mu\text{m}$  hole. This geometry provides a “closed” ion source configuration, allowing at least two orders of pressure differential between the ion source and the analyzer.

The electron beam for the ion source was produced by a tungsten hairpin filament. The filament wire was spot-welded in place on the insulated screws attached to the filament holder and optically aligned over the anode electrode. When the filament burned out, the whole filament assembly was easily detached from the anode and replaced by an already mounted spare filament, avoiding the need to perform a critical alignment in the field. The electron beam current passing through the slits on both the top and bottom of the ionization chamber could be monitored via a trap electrode.

The most important element of the whole construction process for the miniature mass spectrometer was the design and fabrication of the small 90° cylindrical electric sector, in which microfabricated copper-clad alumina were used to control the electric field inside the analyzer. Without any correction of the electric fringing field effect, adequate double focusing of the ion beam by the miniature  $ExB$  analyzer cannot be achieved. In order to correct the electric field distortions at the top and bottom of the sector electrodes, the appropriate potentials needed to be independently established at the radial gap between the opposing edges of the electrodes. This was accomplished by placing at the top and bottom of the radial gap an array of intermediate electrodes, each of which was a circular segment with the same axis as the cylindrical electrodes. Each individual electrode was set to a voltage  $V_n$  varying logarithmically with  $r$ , thus creating the same  $1/r$  electric field dependence, which would exist if the cylinders were infinite in height. The appropriate number of electrodes was established using the finite element model again. We found that 9 equally spaced electrodes with a width of 100  $\mu\text{m}$  were able to provide adequate electric fringing field corrections (Figure 10).

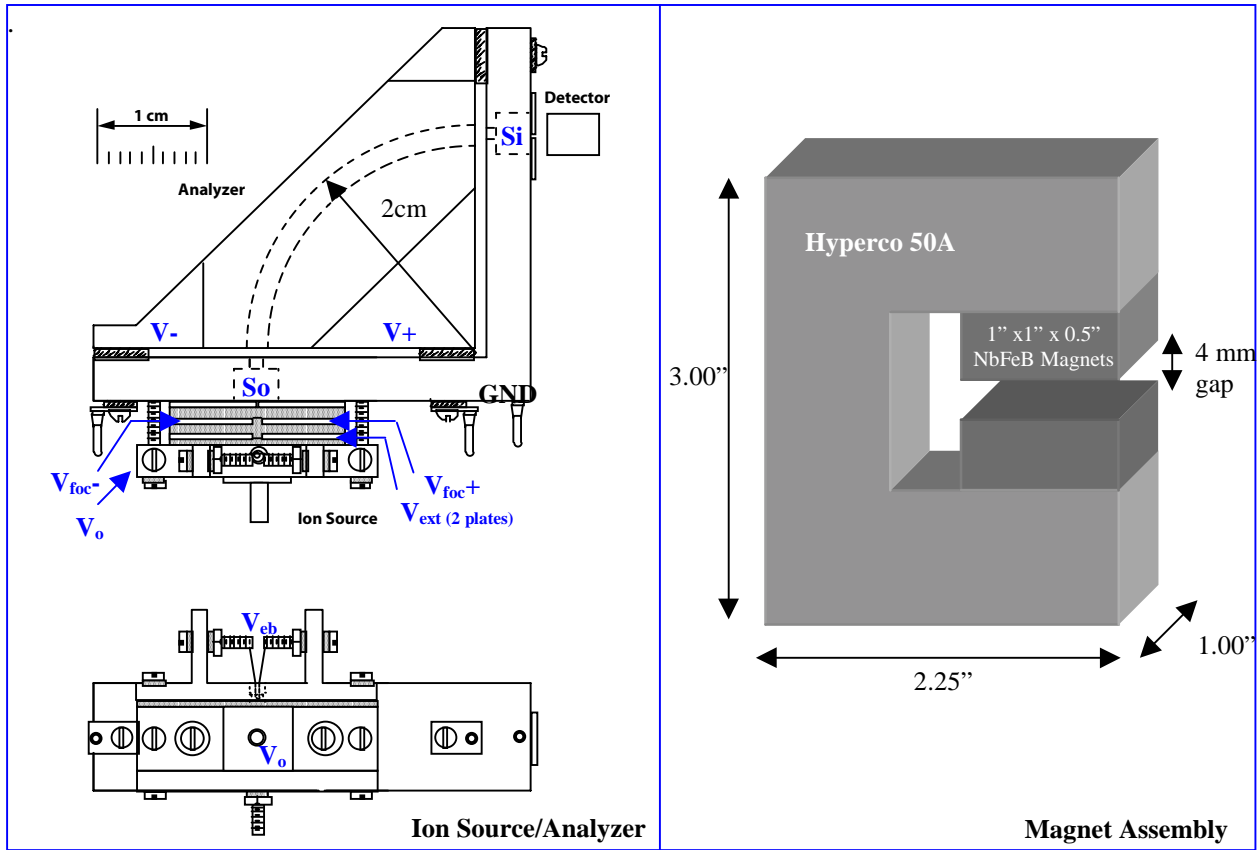


Figure 9: Compact Double Focusing Mass Spectrometer Prototype Design

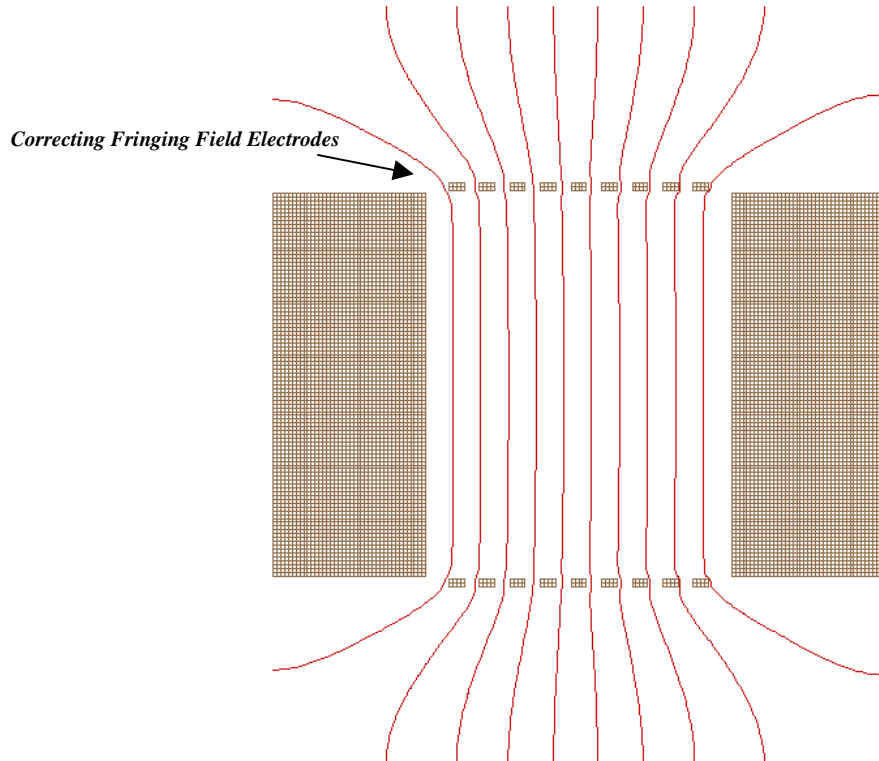


Figure 10. SIMION 3D Ion Simulation: Electric Fringing Field Effects Correction ExB Analyzer Cross Section

The circular segment array of “fringing field” electrodes was formed lithographically on 0.5 mm thick copper clad alumina. On the opposite side of each electrode plate, an array of voltage divider resistors was lithographically deposited and each was laser trimmed to the desired resistance, (Figure 11).

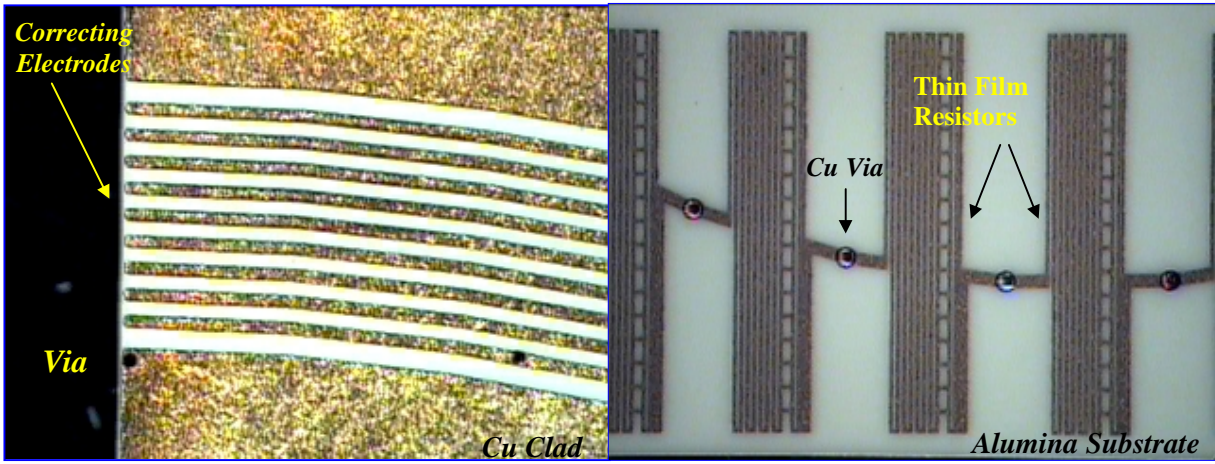
The inner and outer cylindrical electrodes were fabricated from copper plate by conventional NC machining methods. Assembly was done using 2 mm sapphire balls to align the cylindrical electrodes all along the radial gap. Each of the copper clad alumina plates was then attached to the cylindrical electrodes using a silver based conductive epoxy, and aligned optically until both the correcting and the cylindrical electrodes had the same center axis. To protect the resistor network from scratches, the resistor side was coated with a thin film (0.1mm) of hard epoxy. The thickness of the entire resulting assembly was still smaller than the 4 mm magnet gap.

The next step in the construction of the CDFMS prototype was the mounting of the ion detector. The detector used was a Micro-Channel Plate (MCP) particle multiplier from Galileo Corporation<sup>(32)</sup>. We used the smallest standard MCP available from Galileo, having dimensions of 11mm x 12mm and 1.1 mm thick, which was much bigger than the active area required by the mass spectrometer.

The ion source, mass analyzer and detector were all mounted on the same “L” shaped metal bracket. The three components together constituted the core of our miniature mass spectrometer, depicted in Figure 1. The size of the CDFMS core was just 4cm x 3.5cm x 1cm, which is considerably smaller than any double focusing mass spectrometer described in the literature.

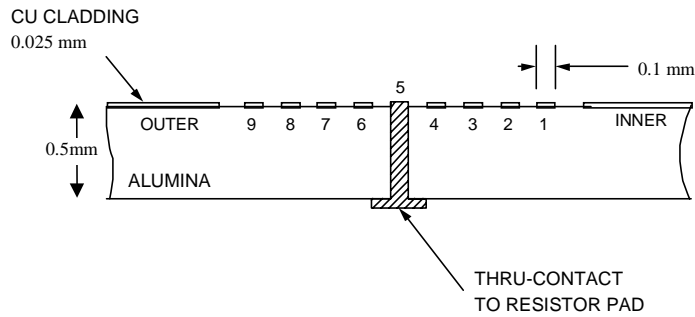
The MCP offered the advantages of fast response, high gain and low noise, as well as a high maximum operating temperature (350°C). In addition, it has been demonstrated<sup>(33)</sup> that such MCP detectors are able to operate at relatively high pressures (10 mtorr) which makes them potentially compatible with relatively simple vacuum systems for portable applications. The MCP was placed inside a machined fixture that provided electrical connections to the external bias voltage, as well as shielding from any external source of radiation or current.

The magnetic field was established by two rare-earth neodymium iron boron (NdFeB) permanent magnets with high energy product (48MGO)<sup>(34)</sup>, mounted on a ferromagnetic yoke made of vanadium cobalt iron (VCoFe) alloy ( $\mu_m = 2000$  G/Oe) known as Hyperco 50A<sup>(35)</sup>. Its construction, design and materials were selected in such way to achieve a very high magnetic flux density, while avoiding the saturation of the magnetic circuit and consequent flux leakage. The field obtained was 1.07 Tesla. These magnets also have high resistance to demagnetization, and can be used at temperatures up to 150°C, which is important for environmental applications. We also found that ordinary cold rolled steel as the yoke material was almost as good as the very expensive VCoFe alloy. The field obtained with such yoke was 0.98 Tesla.



a) ERF Correcting Electrodes

b) Resistor Network



c) Cross Section

Figure 11. Analyzer Plate Microfabrication

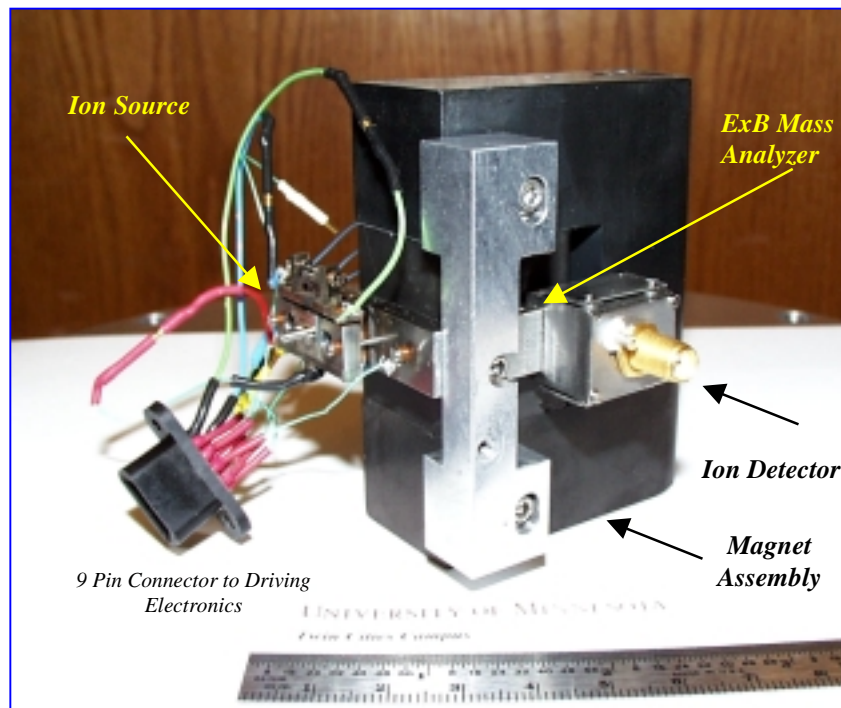


Figure 12. Compact Double Focusing Mass Spectrometer Prototype

An aluminum fixture was used to attach the mass spectrometer core to the magnet assembly. Figure 12 shows the entire CDFMS prototype. The overall size of this first instrument, including the magnet assembly, was approximately  $3.5\text{cm} \times 6\text{cm} \times 7.5\text{cm} = 157.5\text{ cm}^3$  and its weight was less than 0.8 kg.

#### IV Lab Testing and Results

For testing, the mass spectrometer was mounted on an aluminum flange that provided all the necessary electrical and gas feed-through connections and was put into a diffusion-pumped vacuum chamber having a background pressure of  $5.0 \times 10^{-7}$  torr. The 0.076 mm dia. tungsten filament furnished  $10\mu\text{A}$  of emission current with a heating current of 0.9A and a power consumption of 2 W.

In a series of mass spectra measured for residual gases, the optimum voltage ratios for the extractor and focussing electrodes were experimentally determined and found to be in good agreement with the values found in the computer simulations. The same was true for the inner and outer cylindrical electrode voltages. As suggested by the computer model, all the electrode voltages are proportional to a single scanning voltage  $V$ , thus requiring only one control voltage to be scanned in producing a mass spectrum. The CDFMS prototype was able to detect the common residual gas species present in the diffusion pump vacuum system, including oil peak clusters from hydrocarbons up to 100 amu, as shown in Figure 13.

The first CDFMS prototype was equipped with 0.2mm slits, so as to provide a theoretical resolving power of around 100 FWHM. The corresponding value determined experimentally for the nitrogen peak ( $m/z = 28$  amu) was 92.3. The background gas measurements demonstrated a dynamic range of about 5 orders of magnitude and a residual gas detection sensitivity of about 10 ppm with the single-stage MCP detector.

The next characterization test performed was the detection of gas samples introduced into the miniature mass spectrometer through a molecular flow leak inlet. There are several advantages for using a molecular flow inlet<sup>(36)</sup> to inject an atmospheric-pressure sample directly into the ionization chamber (usually at an operating pressure of  $10^{-4}$  torr). First, the sample can be introduced without the use of a bypass flow arrangement or an auxiliary pump. Second, the flow of the individual gases through the inlet is independent of the composition and relative concentration of species in the sample. Our molecular flow leak inlets were constructed from sintered stainless steel frits commercially available from Mott Corporation<sup>(37)</sup>. For our application, we specified a conductance of 15 standard cubic centimeters per minute (sccm) at 1500 psi differential pressure across the material. The frit was placed in a special machined stainless steel holder and sealed radially using an O-ring.

**CDFMS Experimental Mass Spectrum**  
**Residual Gas Analysis: Diffusion Pump Vacuum System**

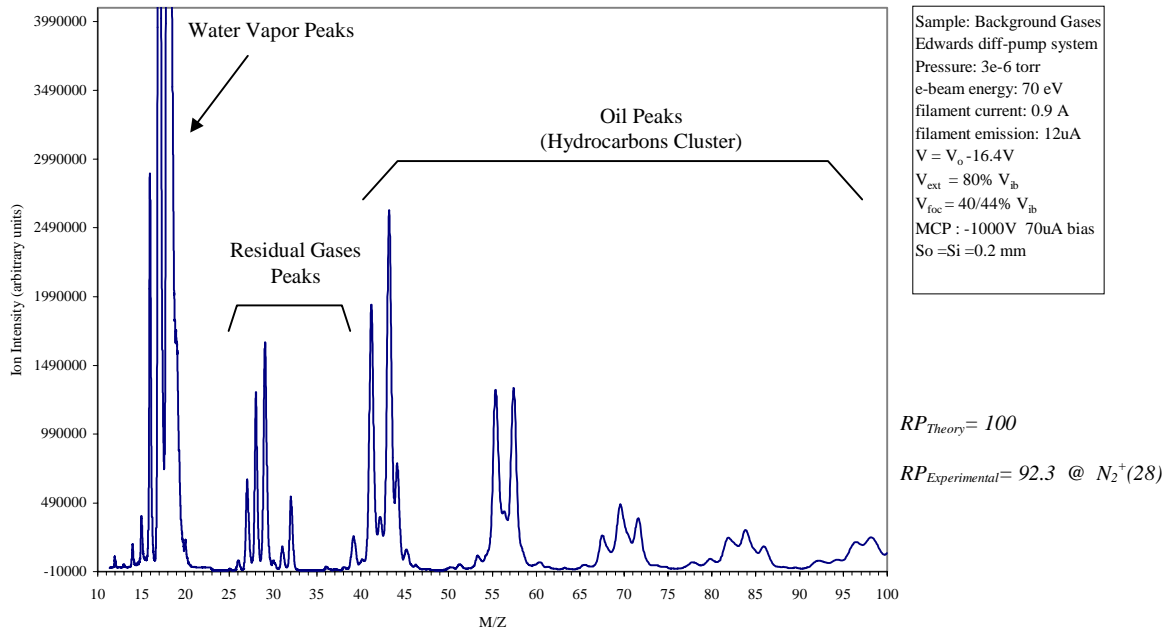


**Figure 13. Mass Spectra: Residual Gas Analysis of Diffusion Pump Vacuum System**

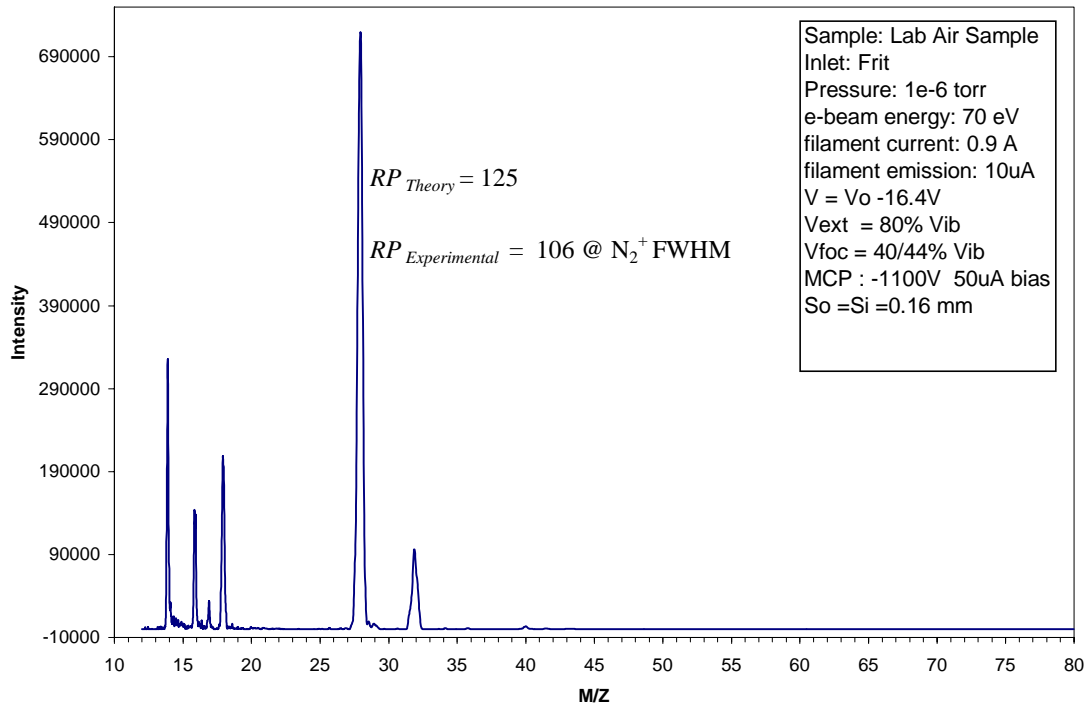


**Figure 14. CDFMS Mass Spectrum: Laboratory Air Sample. Molecular Frit Inlet.**

This fixture provided a cap that had a soldered male Luer-lock<sup>®</sup> adapter to connect a needle, and a teflon valve for laboratory gas analysis. The other side of the frit holder was connected to the vacuum chamber gas feedthrough. Lab air could then be sampled by simply opening the teflon valve.

Figure 14 shows the mass spectrum obtained with the CDFMS for lab air sampled through the molecular flow inlet assembly. These measurements were made with slit widths of 0.16mm., For this slit width, the theoretical maximum resolving power is 125. The experimental value measured at the  $N_2^+$  ion peak was 106. The miniature mass spectrometer was able to detect fully the expected ion peaks from the main gas molecules present in the air sample. The inlet assembly and “closed” ion source design provided a pressure about a factor of 100 higher inside the ionization chamber than in the rest of the vacuum system. In this way, the ion signal was increased and the concentrations of the background gases were negligible compared to the concentration of the sampled gas species coming through the inlet. Some water vapor was detected ( $H_2O^+$  and  $OH^+$  ion peaks in Figure 15), probably coming from the vacuum and inlet systems, due to the fact that they were not purged of residual water.

To determine the effective mass range of the instrument, a sample of Freon 11 ( $Cl_3FCH_4$ ) vapor was introduced through the molecular flow inlet. As a standard for comparison, the mass spectrum of the Freon 11 sample was also measured with a commercial mass spectrometer, a Stanford Research Systems QMS-300. Figure 16 shows both spectra, confirming that the miniature mass spectrometer was able to detect and resolve ion peaks with mass-to-charge ratios up to 103 amu. Differences in the peak intensities in the two spectra are the result of different peak shapes and different mass-dependent transmission efficiencies for the two types of analyzer, either of which must be carefully calibrated for quantitative measurements. It is clear, however, that the CDFMS prototype is capable of performing analyses of atmospheric gas components up to 100 amu, which is sufficient for many environmental monitoring applications.

## V. Discussion and Future Work

In exploring further the limitations of the prototype CDFMS design, the experiments described above were repeated with 0.10 mm analyzer slit widths. Although the computer simulations predicted  $RP = 190$  for the narrower slits, this time it was not possible to measure any higher experimental resolving power than was obtained with 0.16 mm slits. We believe the explanation likely lies in magnetic field inhomogeneity and fringing field details which are not fully incorporated into the computer model at present.

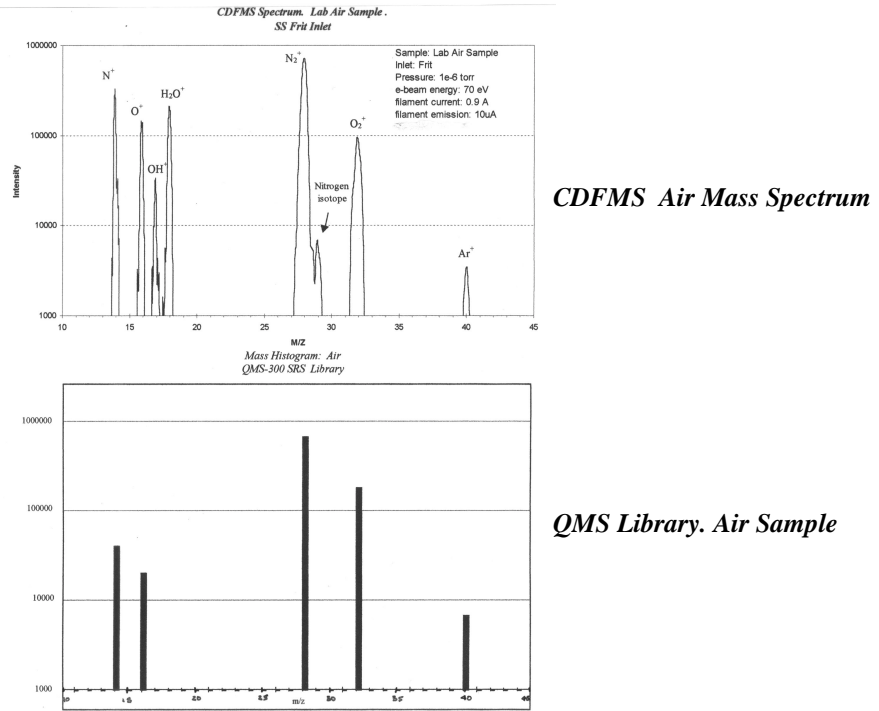


Figure 15: Mass Spectrum: Lab Air Sample. Log Scale Comparison with QMS Library

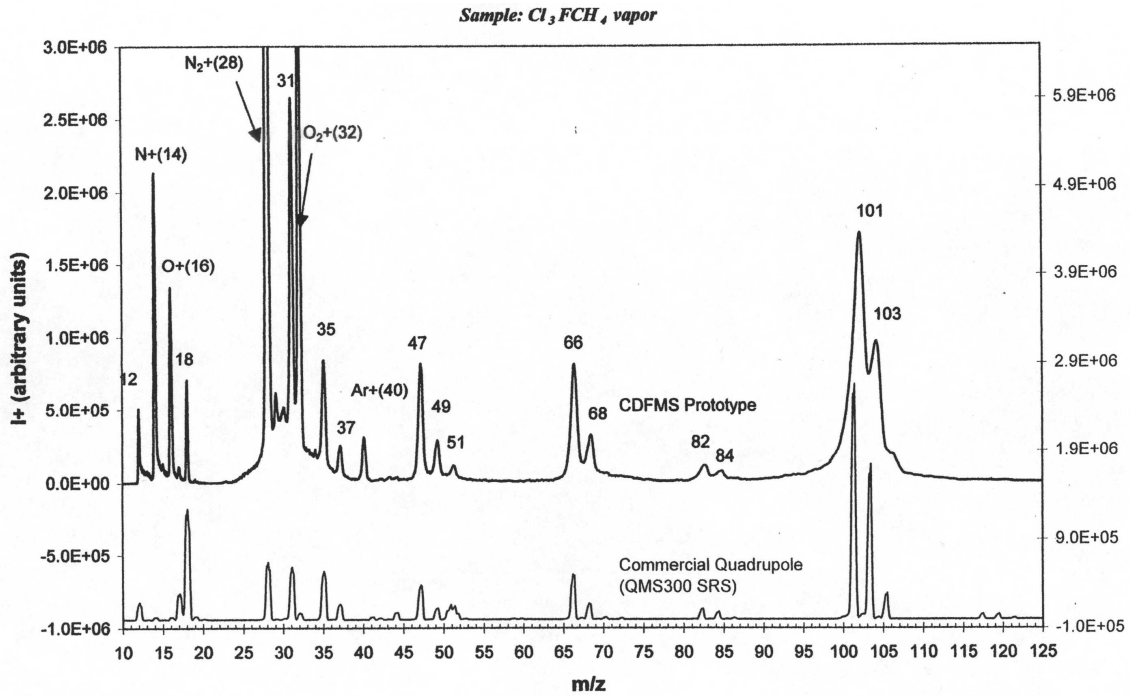


Figure 16. CDFMS Mass Range Test. Commercial QMS vs Prototype Spectra

As mentioned above, double focusing of a particular  $m/z$  requires a ratio of magnetic force to electric force of  $-2$  along the entire ion path through the crossed sector field analyzer. With a variation in the magnetic field along the ion path, this ratio cannot be maintained exactly with the present electric sector design. Future work will be directed toward shaping the electric field to match the corresponding magnetic field at each point along the ion path between the two analyzer slits.

To further increase the sensitivity of the CDFMS, we plan to substitute a sub-miniature channeltron-style multiplier for the microchannel plate multiplier. The gain with this new detector is predicted to be as high as  $10^6$ , which is 100 times higher than the one used in the experiments described above. With the new detector, the CDFMS should be capable of detecting gas concentrations of about 0.1 ppm, but more testing will need to be done to verify this possibility.

The finite element model and ion trajectory simulations provided a very practical and inexpensive method for testing the design ideas and optimizing operating parameters for the first CDFMS to be constructed. We are gratified that the experimental performance was predicted so well by a relatively simple computer model. One application which we envisioned from the beginning of this project is on-site monitoring of volcanic gaseous emissions, which occur at many sites around the world, including Costa Rica and several western states in the U.S. From these first results, we conclude that the CDFMS prototype design is able to detect all of the important gas molecules present in volcanic gaseous emissions. The construction of a portable vacuum system and electronics package suitable for such testing is underway, and the results of such experiments will be presented in a later paper.

Looking further ahead, one can envision a miniature mass spectrometer constructed solely by microfabrication techniques, to lower the construction time and cost as well as to perform alignment and fringing field corrections that are more difficult to do with conventionally-machined and manually assembled electrodes. The design of such device has already been done<sup>38</sup> incorporating its own vacuum envelope to minimize the gas volume to be pumped out.

## **VI Acknowledgments and Disclosures**

We would like to thank the University of Minnesota for financial support of this research. The project was financed by the Microtechnology Laboratory through Research Initiative #200 and by a similar initiative from the Academic Health Center

We also thank the Graduate School of the University of Minnesota for a Grant-in-Aid. JAD wishes to express his appreciation to the Fulbright-Laspau Program and the University of Costa Rica for awarding him a fellowship to conduct his doctoral studies at UM.

A U.S. patent application has been filed which covers the intellectual property generated in the course of this research project. As inventors, JAD, CFG and WRG are all participants in the University of Minnesota's royalty-sharing policy. In addition, WRG is a consultant to and shareholder of Mass Sensors, Inc, a private company to which this technology has been licensed by the University of Minnesota.

## VII Bibliography

- <sup>1</sup> J.A. Diaz. Sub-miniature double-focusing mass spectrometer for in-situ environmental monitoring and application to volcanic gaseous emissions. *Ph.D. Thesis. University of Minnesota, July 1999.*
- <sup>2</sup> H.E Duckworth et. al, *Mass Spectroscopy, Cambridge University Press, 2<sup>nd</sup> Ed.*, p.8, 1986
- <sup>3</sup> W. Wien, *Annalen der Physik, Leipzig*, v.8, p.224, 1902
- <sup>4</sup> A. O. Nier, J. L. Hayden, "A miniature Mattauch-Herzog mass spectrometer for the investigation of planetary atmospheres", *International Journal of Mass Spectrometry*, v.6. n.5-6, p.339, 1971.
- <sup>5</sup> J. P. Carrico, et. al., "Miniature Mattauch-Herzog mass spectrometer", *Journal of Physics E- Scientific Instruments*, v.7, no.6, 1974
- <sup>6</sup> M. P. Sinha and A. D. Tomassian, "Development of a miniaturized, light-weight magnetic sector for a field-portable mass spectrograph", *Review of Scientific Instruments*, v.62, n.11, p.2618, 1991
- <sup>7</sup> W. Bleakney and J. A. Hipple. *Physical Review*, v.53, p.521, 1938
- <sup>8</sup> L. G. Smith, *Physical Review*, v.81, p.295, 1951
- <sup>9</sup> D. L. Swinger, "A small magnetic analyzer mass spectrometer with a velocity Wein filter for residual gas analysis" *Vacuum*, v. 21, n. 3-4, p.121. 1971
- <sup>10</sup> C. F. Robinson and L. G. Hall, "Small general purpose cycloidal-focusing mass spectrometer", *Review of Scientific Instruments*, v. 27, n.7, p.504, 1956
- <sup>11</sup> D. L. Swinger, "A compact helium detector", *International Journal of Mass Spectrometry and Ion Physics*, v.17, p.321, 1975
- <sup>12</sup> H. F. Hemond, "A backpack-portable mass spectrometer for measurements of volatile compounds in the environment", *Review of Scientific instruments*, v.62, n.6, p.1420, 1991
- <sup>13</sup> W. Bartky and A. J. Dempster, "Paths of charged particles in electric and magnetic fields", *Physical Review*, v.33, p1019, 1929
- <sup>14</sup> Von H. Bondy and K. Popper, "Ein Massenspektrometer mit Richtungs- und Geschwindigkeitsfokussierung" *Annalen der Physik*. v.17, p.425, 1933
- <sup>15</sup> Von H. Bondy, G. Johannsen and K. Popper, "Über die raltiven Haufigkeiten der Isotope von Kalium und Rubidium" *Zeitschrift fur Physik*. v.95, p.46, 1935
- <sup>16</sup> Von D. Fischer., "Fokussierungseigenschaften einer Kombination aus einem mit dem radius abfallendem magnetfeld und einem elektrischen Zylinderfeld", *Zeitschrift fur Physik*, v.133, p.455, 1952
- <sup>17</sup> Von D. Fischer, "Ein Massenspektrometer mit doppelter Richtungs- und Geschwindigkeitsfokussierung", *Zeitschrift fur Physik*, v.133, p.471, 1952
- <sup>18</sup> H. Matsuda, "Mass spectrometer with superimposed electric and magnetic fields", *US Patent 3984682*, Oct 5, 1976
- <sup>19</sup> H. Matsuda, "Mass spectrometer with crossed electric and magnetic fields", *Mass Spectroscopy*, v.21, p.4, 1973
- <sup>20</sup> H. Matsuda, M. Naito, et al., "Constant accelerating voltage electric-field scanning mass spectrometer", *Advances in Mass Spectrometry*, n.7b, p.846, 1976
- <sup>21</sup> H. Matsuda, "Electrostatic analyzer with variable focal length", *Review of Scientific Instruments*, v.32, n.7, p.850, 1961
- <sup>22</sup> H. Matsuda and Y. Fujita, "Potential distribution in a cylindrical condenser terminated by Matsuda plates ", *International Journal of Mass Spectrometry and Ion Physics*, v.16, p.395, 1975
- <sup>23</sup> F. Kunihiro, M. Naito, Y. Naito. "A new MS/MS with crossed  $ExB$  field as the second analyzer", *32<sup>nd</sup> Annual Conference on Mass Spectrometry and Allied Topics: Retrospective Lectures*, p.523, 1984
- <sup>24</sup> M. Naito, "Mass spectrometer with superimposed electric and magnetic fields", *US Patent 4054796*, Oct 18, 1977

- 
- 25 J. A. Diaz, W. R. Gentry and C. F. Giese, "Double focussing mass spectrometer apparatus and methods regarding same", *Patent Application, University of Minnesota*, Docket No. 96035, 1999
- 26 J. Mattauch and R. Herzog, *Annalen der Physik*, v.19, p.345, 1934
- 27 J. Mattauch and R. Herzog, *Zeitschrift für Physik*, v.89, p.789, 1934
- 28 R. W. Gentry, "Notes on Crossed Field Selectors", *personal notes (unpublished)*, 25 Oct 1971
- 29 David A. Dahl. SIMION 3D version 6.0. *Idaho National Engineering Laboratory*. P.O Box 1625 Idaho Falls, ID 83415
- 30 H. Matsuda, Double-focusing mass spectrometer of short path length, *International Journal of Mass Spectrometry and Ion process*, v.93, p.315, 1989
- 31 Precision Air Slit. Part Number: H38560. Edmund Scientific Company. Industrial Optics Division. 101 East Gloucester Pike. Barrington, NJ, 08007
- 32 Long Life Micro Channel Plate. Part Number:1393-1200. *Galileo Corporation P.O Box 550. Sturbridge, MA 01566*
- 33 B. Laparade and R. Cochran. "Performance and Characterization of a Sub-Miniature Microchannel Plate Detector in a Mass Spectrometer Application". *Pittcon 1998 Presentation. Galileo Corporation. P.O Box 550. Sturbridge, MA 01566*
- 34 Neodymium Iron Boron Block. Part Number: CM40729-3714 and PN48R0100B. Dexter Magnetic Materials Division. 1050 Morse Ave. Elk Grove Village, IL 60007.
- 35 Hyperco 50A. *Carpenter Technology Corporation. 101 W. Bern St. Reading, PA 19612*
- 36 G. V. Moore and B. W. Scott. Final Report Inlet Leak Study. *The Perkin-Elmer Corporation Aerospace Division. v.4, p.1, 1971*
- 37 Sintered SS Frit. Part Number: 5010793. *Mott Corporation 84 Spring Lane, Farmington, CT 06032*
- 38 J. A Diaz. "Design, Modeling and Process Module of a Micro-Fabricated Mass Spectrometer on a Chip for Analytical Applications" *MSEE Thesis*. University of Minnesota, 1998